Supporting Information

NiCo@NPC@CF nanocomposites derived from NiCo-MOF/cotton for electromagnetic wave absorption

Hongdu Jin[a] & Hui-Min Wen[a], Qu Hong[a], Jun Lin[a], Jun Li[a] and Jun Hu*[a]*

[a] College of Chemical Engineering, Zhejiang University of Technology, Hangzhou 310014, P.R. China

E-mail: huiminwen@zjut.edu.cn; hjzjut@zjut.edu.cn.

Table S1 The dielectric loss of samples

Sample	Frequency (GHz)[a]	ε_c''	ε_p''	$\varepsilon_c''/\varepsilon_p''$
NiCo@NPC@CF-600	6.08	0.391	1.496	0.261
NiCo@NPC@CF-700	6.72	0.354	2.627	0.135
NiCo@NPC@CF-800	9.36	0.254	9.230	0.028

[a] Frequency at RLmin.
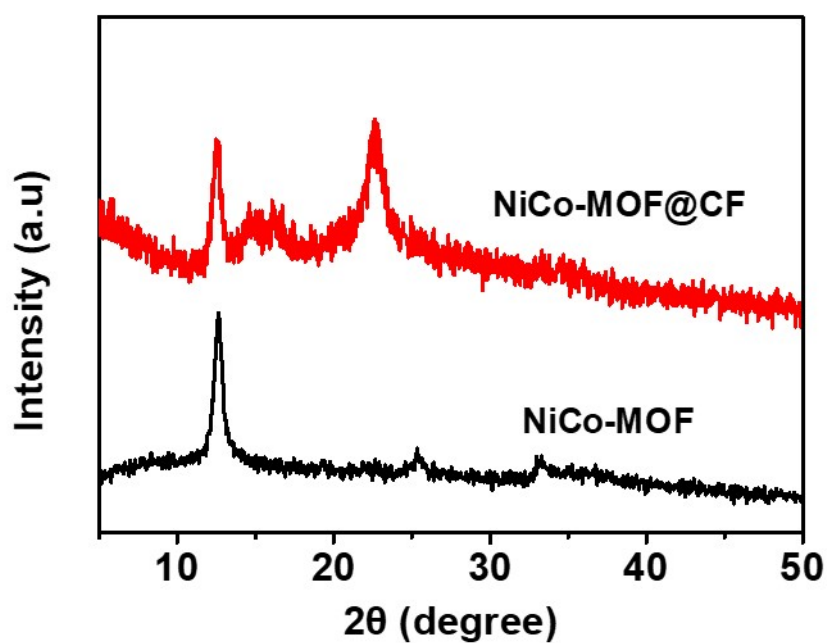
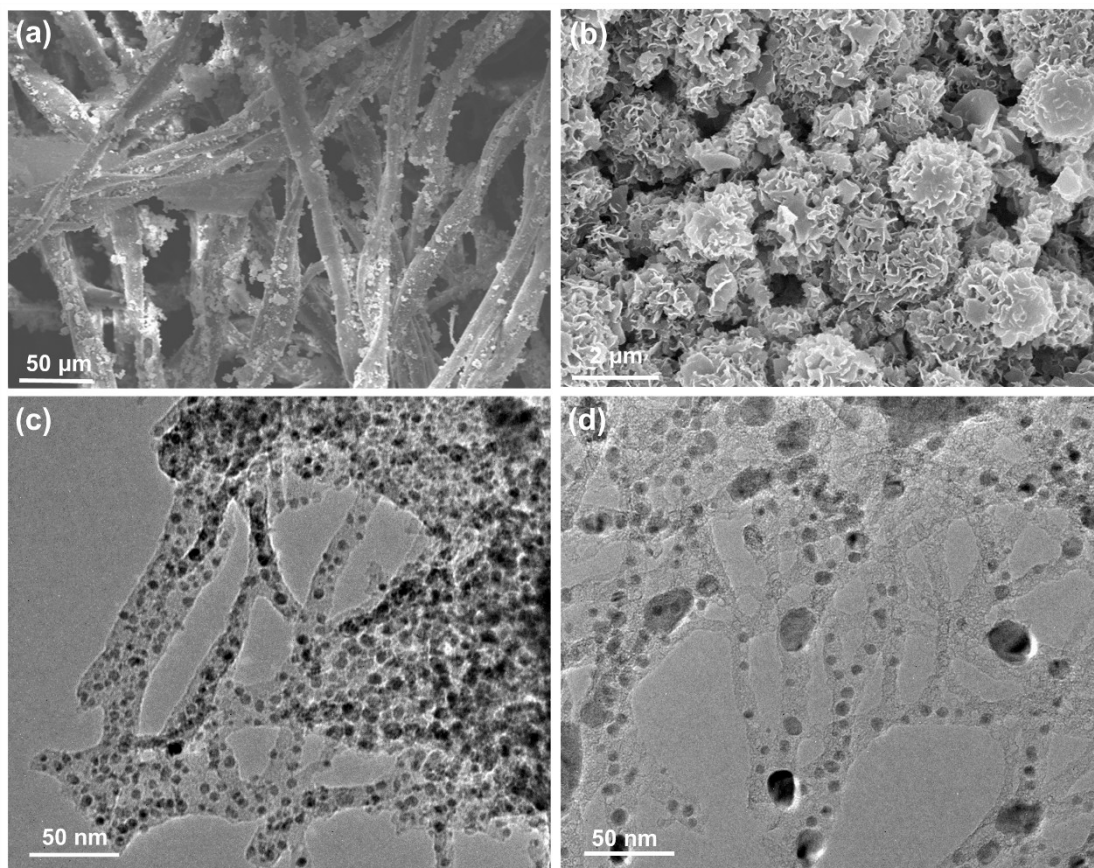**Fig. S1.** XRD patterns of NiCo-MOF and NiCo-MOF@CF.

Fig. S2. SEM images for NiCo-MOF coated cotton fiber precursor NiCo-MOF@CF (a,b), TEM images for NiCo@NPC@CF-600 (c) and NiCo@NPC@CF-800 (d).
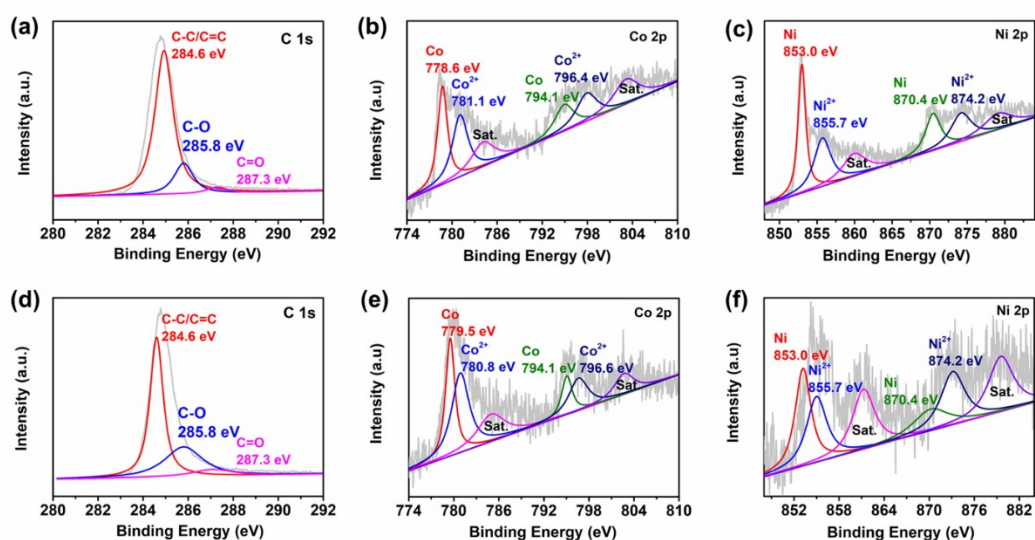

Fig. S3. XPS spectra of for NiCo@NPC@CF-600: (a) C 1s, (b) Co 2p, (c) Ni 2p, and for NiCo@NPC@CF-800: (d) C 1s, (e) Co 2p, (f) Ni 2p.
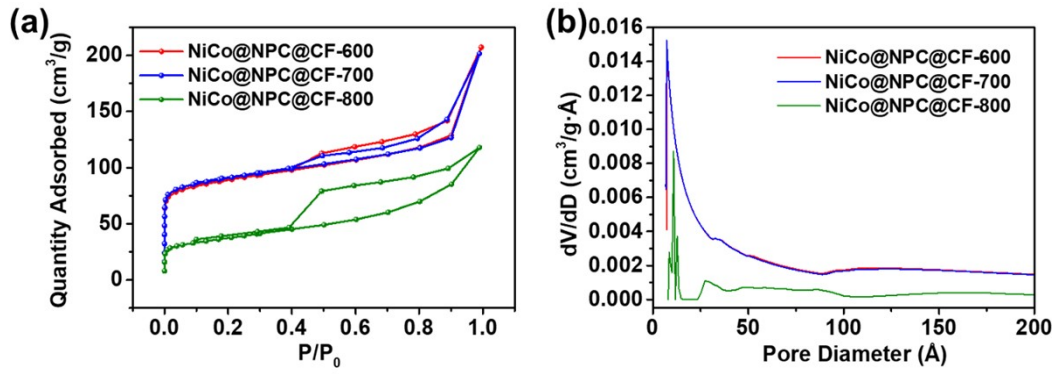
Fig. S4. (a) N$_2$ adsorption-desorption isotherms, and (b) Pore-size distributions derived from the adsorption branch by the BJH method of NiCo@NPC@CF-600, NiCo@NPC@CF-700 and NiCo@NPC@CF-800.
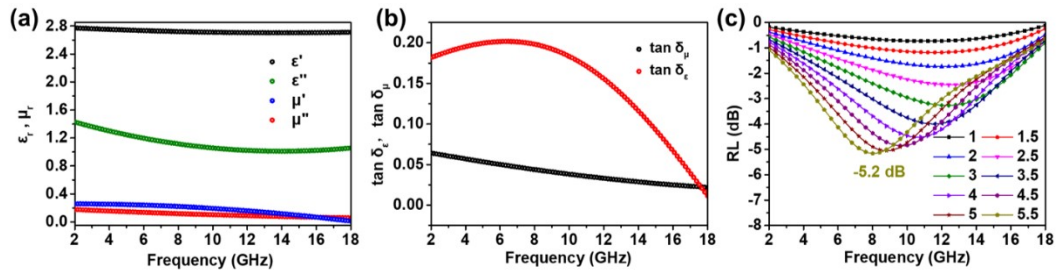

Fig. S5. Complex permittivity and permeability (a), dielectric loss tangent and magnetic loss tangent(b) and Reflection loss curves (c) for NiCo@NPC-700.
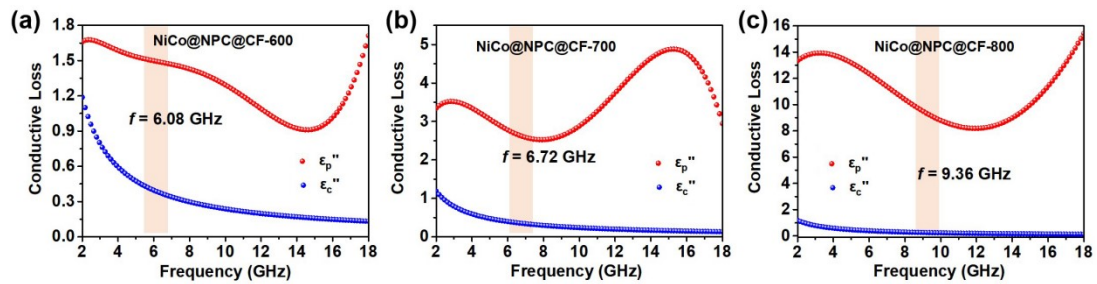

Fig. S6. Plots of ε_c'' and ε_p'' vs frequency: (a) NiCo@NPC@CF-600, (b) NiCo@NPC@CF-700 and (c) NiCo@NPC@CF-800.
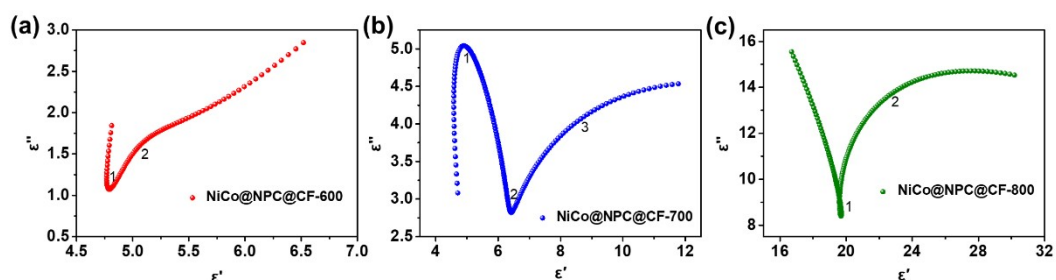
Fig. S7. The cole–cole plots of (a) NiCo@NPC@CF-600, (b) NiCo@NPC@CF-700 and (c) NiCo@NPC@CF-800.
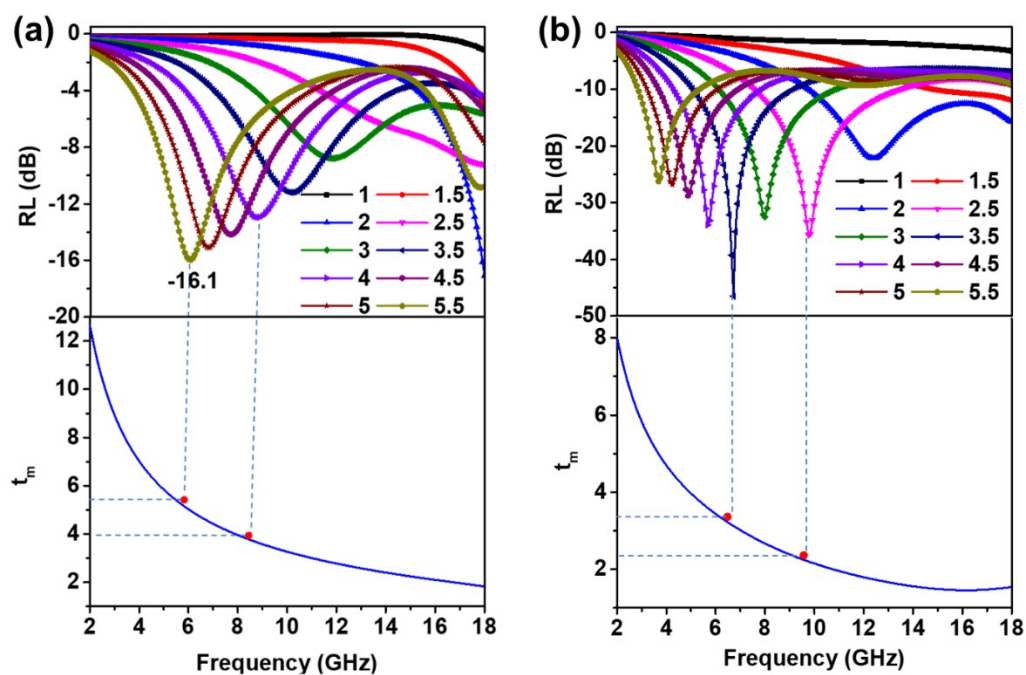

Fig. S8. The relationship between thickness and peak frequency of (a) NiCo@NPC@CF-600 and (b) NiCo@NPC@CF-700 derived from the quarter-wavelength cancellation model.
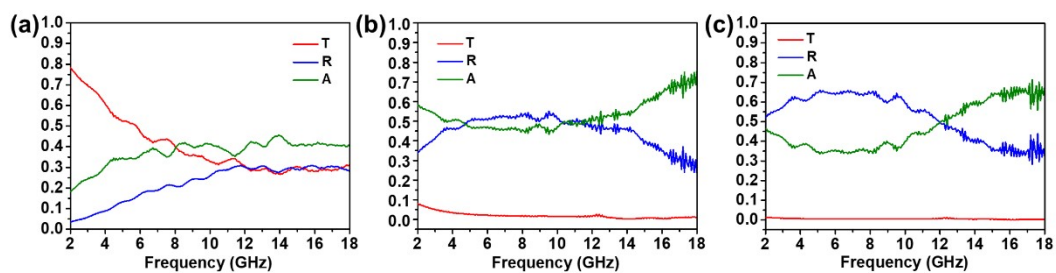

Fig. S9. The corresponding R, A, and T values of (a) NiCo@NPC@CF-600, (b) NiCo@NPC@CF-700 and (c) NiCo@NPC@CF-800.